AGU PUBLICATIONS

JGR

Journal of Geophysical Research: Space Physics

RESEARCH ARTICLE

10.1002/2016JA022447

**Special Section:**
Inner Magnetosphere Coupling: Recent Advances

**Key Points:**
- The effects of wave growth and damping are considered to generalize the conventional ULF wave-particle drift resonance theory
- Particle signatures are predicted to be very different from the characteristic 180 degree phase shift of particle fluxes across energies
- Newly predicted particle signatures are consistent with Van Allen Probe observations, which validate the generalized theory

**Correspondence to:**
X.-Z. Zhou,
xzzhou@pku.edu.cn

**Citation:**
Zhou, X.-Z., Z.-H. Wang, Q.-G. Zong, R. Rankin, M. G. Kivelson, X.-R. Chen, J. B. Blake, J. R. Wygant, and C. A. Kletzing (2016), Charged particle behavior in the growth and damping stages of ultralow frequency waves: Theory and Van Allen Probes observations, *J. Geophys. Res. Space Physics*, *121*, 3254–3263, doi:10.1002/2016JA022447.

Received 27 JAN 2016
Accepted 28 MAR 2016
Accepted article online 31 MAR 2016
Published online 25 APR 2016
Corrected 23 AUG 2016

This article was corrected on 23 AUG 2016. See the end of the full text for details.



# Charged particle behavior in the growth and damping stages of ultralow frequency waves: Theory and Van Allen Probes observations

**Xu-Zhi Zhou[1,2], Zi-Han Wang[1], Qiu-Gang Zong[1,2], Robert Rankin[3], Margaret G. Kivelson[2,4], Xing-Ran Chen[1], J. Bernard Blake[5], John R. Wygant[6], and Craig A. Kletzing[7]**

[1]School of Earth and Space Sciences, Peking University, Beijing, China, [2]PKU/UCLA Joint Research Institute in Science and Engineering,, [3]Department of Physics, University of Alberta, Edmonton, Alberta, Canada, [4]Department of Earth, Planetary, and Space Sciences, University of California, Los Angeles, California, USA, [5]Space Science Applications Laboratory, The Aerospace Corporation, El Segundo, California, USA, [6]School of Physics and Astronomy, University of Minnesota, Twin Cities, Minneapolis, Minnesota, USA, [7]Department of Physics and Astronomy, University of Iowa, Iowa City, Iowa, USA

**Abstract** Ultralow frequency (ULF) electromagnetic waves in Earth's magnetosphere can accelerate charged particles via a process called drift resonance. In the conventional drift resonance theory, a default assumption is that the wave growth rate is time independent, positive, and extremely small. However, this is not the case for ULF waves in the real magnetosphere. The ULF waves must have experienced an earlier growth stage when their energy was taken from external and/or internal sources, and as time proceeds the waves have to be damped with a negative growth rate. Therefore, a more generalized theory on particle behavior during different stages of ULF wave evolution is required. In this paper, we introduce a time-dependent imaginary wave frequency to accommodate the growth and damping of the waves in the drift resonance theory, so that the wave-particle interactions during the entire wave lifespan can be studied. We then predict from the generalized theory particle signatures during different stages of the wave evolution, which are consistent with observations from Van Allen Probes. The more generalized theory, therefore, provides new insights into ULF wave evolution and wave-particle interactions in the magnetosphere.

## 1. Introduction

Transverse electromagnetic oscillations in the ultralow frequency (ULF) Pc4–5 bands (between 2 and 22 mHz) are usually found in the Earth's magnetosphere to be hydromagnetic waves standing on closed geomagnetic field lines [e.g., *Cummings et al.*, 1969; *Chen and Hasegawa*, 1974; *Southwood*, 1974; *Singer et al.*, 1982; *Takahashi and McPherron*, 1984; *Hartinger et al.*, 2011]. These ULF waves, especially the poloidal mode ULF waves with electric field oscillations in the azimuthal direction, can modulate energetic particle fluxes in the magnetosphere [*Kokubun et al.*, 1977; *Zong et al.*, 2009; *Claudepierre et al.*, 2013; *Foster et al.*, 2015]. Because energetic particles drift mainly in the azimuthal direction, they can be either accelerated or decelerated by the ULF waves. Particles that drift at the same azimuthal speed as the waves may even experience a stable electric field, which leads to a net energy excursion. This process is known as wave-particle drift resonance [*Southwood and Kivelson*, 1981, 1982], a major candidate for acceleration of particles in the Van Allen radiation belt [*Mann et al.*, 2013]. Such resonance may also occur between energetic particles and toroidal ULF waves (with electric field oscillations in the radial direction) due to the radial component of particle drift motion associated with noon-midnight asymmetry of the geomagnetic field [*Elkington et al.*, 2003; *Zong et al.*, 2007].

According to the drift resonance theory [*Southwood and Kivelson*, 1981], for resonant particles, the flux observed at a fixed location would oscillate at a large amplitude in antiphase with the azimuthal (eastward) electric field. For particles at lower or higher energies, the amplitude of the flux oscillations would be much smaller, and the corresponding phase difference from the electric field would be ±90°. In other words, particle flux oscillations in different energy channels would shift in phase by 180° across the resonant energy. These characteristic phase relationships, treated as diagnostic signatures of wave-particle drift resonance, have been clearly identified from Van Allen Probes observations [*Dai et al.*, 2013; *Claudepierre et al.*, 2013; *Hao et al.*, 2014].

A default assumption in the conventional drift resonance theory is that the amplitude of the waves grows extremely slowly. In other words, the imaginary part of the wave angular frequency, Im($\omega$), is time independent, positive, and extremely small. This strict assumption significantly limits wider application of the theory, partially because of the fact that quasi-steady waves in the magnetosphere may have experienced a rapid growth stage when they gain energy from external sources such as the solar wind [*Allan et al.*, 1986; *Lee and Lysak*, 1989; *Mathie and Mann*, 2001; *Kepko et al.*, 2002; *Shi et al.*, 2013] or internal sources such as substorms [*Olson*, 1999; *Hsu and McPherron*, 2007] and ring current ions [*Southwood et al.*, 1969]. In order to accommodate such early-time evolutions of the ULF waves, *Zhou et al.* [2015] applied the drift resonance theory to the regime of large Im($\omega$) and successfully reproduced the nonstandard phase relationships observed immediately after the wave excitation. Moreover, one can expect that after the early growth stage, the ULF waves would eventually be damped [*Glassmeier et al.*, 1984; *Shen et al.*, 2015] requiring negative values of Im($\omega$). Therefore, a generalized theory is required to take into account the time dependence of Im($\omega$) so that particle behavior and characteristic signatures during the entire wave lifespan can be better understood.

It is our goal in this paper to generalize the drift resonance theory. From the generalized theory, we will also predict characteristic particle signatures within different wave stages and then compare them with Van Allen Probes observations. Before presenting our generalization on the drift resonance theory, in the next section, we start with a brief review of the conventional theory given in *Southwood and Kivelson* [1981, 1982].

## 2. Conventional Drift Resonance Theory

Conventional drift resonance theory describes charged particle behavior in transverse ULF wave fields. For a particle of charge $q$ in transverse hydromagnetic waves, its kinetic energy $W$ changes at the average rate

$$\frac{\mathrm{d}W_A}{\mathrm{d}t} = q\boldsymbol{E} \cdot \boldsymbol{v}_d, \tag{1}$$

where the subscript $A$ signifies the average over many gyrations, and $\boldsymbol{v}_d$ is the magnetic gradient and curvature drift velocity of the particle [*Northrop*, 1963]. In Earth's magnetic dipole field, the particle drift velocity $\boldsymbol{v}_d$ can be approximated by

$$\boldsymbol{v_d} = -\frac{3L^2\gamma m_0 v^2}{qB_E R_E}(0.35 + 0.15\sin\alpha_{\mathrm{eq}})\hat{\boldsymbol{e}_\phi}, \tag{2}$$

where $\hat{\boldsymbol{e}_\phi}$ is defined eastward, $R_E$ is Earth's radius, $B_E$ is the equatorial magnetic field on Earth's surface, $L$ is the L shell parameter, $\gamma$ is the relativistic Lorentz factor, $m_0$ is the particle's rest mass, and $\alpha_{\mathrm{eq}}$ is the equatorial pitch angle. In the conventional drift resonance theory [*Southwood and Kivelson*, 1981], the particle is assumed to be nonrelativistic. Therefore, equation (2) becomes

$$\boldsymbol{v_d} = -\frac{6L^2W}{qB_E R_E}(0.35 + 0.15\sin\alpha_{eq})\hat{\boldsymbol{e}_\phi}. \tag{3}$$

The conventional theory also assumes an azimuthal propagation of ULF waves; the wave-associated electric field oscillations are given by

$$\boldsymbol{E} = E_\phi \exp i(m\phi - \omega t)\hat{\boldsymbol{e}_\phi}, \tag{4}$$

where $\phi$ is the magnetic longitude (increasing eastward), $\omega$ is the wave angular frequency (a complex value with a small, positive imaginary part Im($\omega$) representing the gradual growth of the wave amplitude), and $m$ is the azimuthal wave number. For an equatorially mirroring particle, the average rate of its energy change can be derived from equations (1), (3), and (4) to be

$$\frac{\mathrm{d}W_A}{\mathrm{d}t} = -\frac{3L^2W}{B_E R_E} \cdot E_\phi \exp i(m\phi - \omega t), \tag{5}$$

which can be integrated along the particle's drift orbit backward in time to $t = -\infty$ (when the wave amplitude is negligible) to obtain the particle energy gain $\delta W_A$ from ULF waves. In the conventional theory, the particle's orbit is assumed to be unperturbed by the waves despite its energy gain/loss from the ULF waves, so the angular drift frequency $\omega_d$ of the particle is

$$\omega_d = \frac{\mathrm{d}\phi}{\mathrm{d}t} = -3LW/qB_E R_E^2. \tag{6}$$

The integration of equation (5) along the unperturbed orbit (6) then yields the averaged particle energy gain $\delta W_A$:

$$\delta W_A = -i \cdot \frac{3L^2 W}{B_E R_E} \frac{E_\phi \exp i(m\phi - \omega t)}{\omega - m\omega_d}. \tag{7}$$

When drift resonance occurs, $m\omega_d$ equals Re($\omega$), and the denominator of equation (7) becomes Im($\omega$) $\cdot\, i$. This small, imaginary denominator shows that $\delta W_A$ oscillates at a large amplitude in antiphase with the eastward electric field. For particles at lower or higher energies, the smaller or larger $\omega_d$ values imply that the denominator is dominated by its real part (either positive or negative); the corresponding $\delta W_A$ oscillations have much smaller amplitudes and are $\pm 90°$ out of phase with the electric field oscillations. In other words, in this analysis the oscillations of $\delta W_A$ at different energies shift in phase by 180° across the resonant energy.

An actual particle detector cannot measure $\delta W_A$ directly though. To compare these results with observational data, one has to transform $\delta W_A$ into $\delta f_A$ which represents the gyration-averaged change of particle phase space density (PSD). Given the adiabatic response of particles during their interactions with ULF waves, the wave-produced $\delta f_A$ can be written as

$$\delta f_A = -\delta W_A \frac{\partial f(W,\mu)}{\partial W} = \delta W_A \frac{L}{3W} \frac{\partial f(L,\mu)}{\partial L}, \tag{8}$$

where $\mu$ is the first adiabatic invariant. According to *Southwood and Kivelson* [1981], $\delta f_A$ can be alternatively given by

$$\delta f_A = \delta W_A \left[ \frac{L}{3W} \frac{\partial f(W,L)}{\partial L} - \frac{\partial f(W,L)}{\partial W} \right], \tag{9}$$

which also shows that $\delta f_A$ is directly proportional to $\delta W_A$ provided there is a finite PSD gradient in energy and/or space. Therefore, the phase shift of the particle PSD or particle flux across the resonant energy should be also 180°. Such a phase shift is then widely treated as a diagnostic signature of wave-particle drift resonance [*Dai et al.*, 2013; *Claudepierre et al.*, 2013].

Note that the diagnostic signature is valid only for the assumed conditions of extremely slow wave growth. According to equation (7), the phase shift of $\delta W_A$ or equivalently the phase shift of particle fluxes across the resonant energy will be much smaller than 180° if the wave amplitude grows rapidly with a substantial Im($\omega$)/*Re*($\omega$) ratio [*Zhou et al.*, 2015]. Large values of Im($\omega$) may occur during the interval of wave excitation; as time proceeds, however, Im($\omega$) should eventually decrease to negative values during the damping stage of the ULF waves. A time-dependent Im($\omega$) will be introduced in the next section as we generalize the drift resonance theory.

## 3. Generalization

In order to accommodate the growth and damping of the ULF waves in the drift resonance theory, we introduce a linearly decreasing imaginary part of the wave angular frequency:

$$\mathrm{Im}(\omega) = -t/\tau^2, \tag{10}$$

where $\tau > 0$ identifies the time scale of the wave growth and decay. The wave-associated electric field, equation (4), can now be rewritten as

$$\boldsymbol{E} = E_\phi \exp(-t^2/\tau^2) \exp i(m\phi - \omega_r t)\hat{\boldsymbol{e}_\phi}, \tag{11}$$

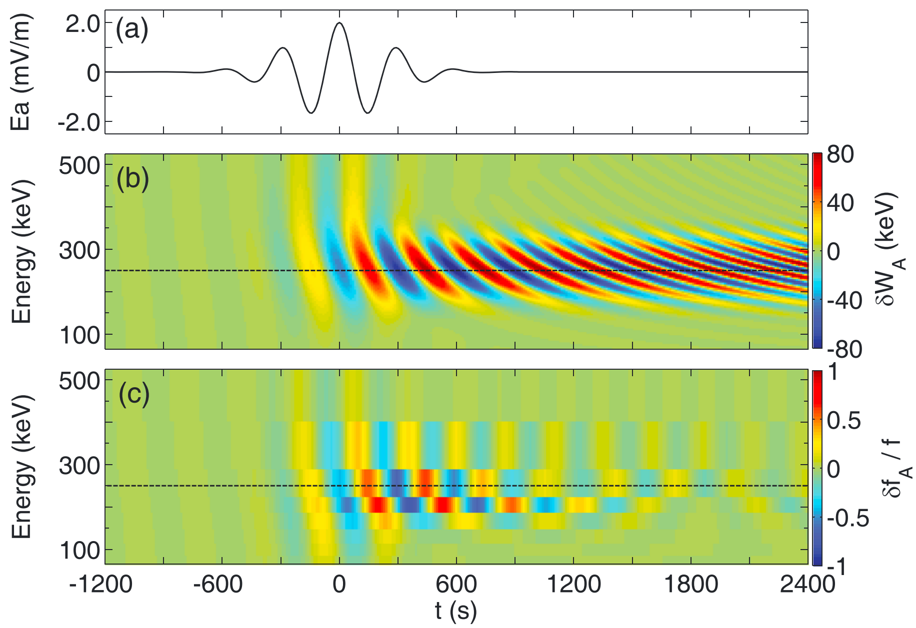


**Figure 1.** Electron responses to a representative ULF wave during its growth and damping stages. (a) ULF wave-associated electric field in the azimuthal direction, (b) electron energy gain from the ULF waves as a function of time and energy, with the resonant energy of 250 keV represented by the dashed line, and (c) predicted spectrum of electron residual phase space densities observed by a Magnetic Electron Ion Spectrometer (MagEIS)-like particle detector with finite time and energy resolution.

where $\omega_r$ represents the real part of the wave angular frequency, $Re(\omega)$. Equation (11) describes a Gaussian envelope of the electric field oscillation amplitude: the wave amplitude grows until $t = 0$ when it starts to decay from its peak. Then we can accordingly rewrite equation (5) to represent the particle's average rate of energy change within these waves:

$$\frac{\mathrm{d}W_A}{\mathrm{d}t} = -\frac{3L^2W}{B_ER_E} \cdot E_\phi \exp(-t^2/\tau^2) \exp i(m\phi - \omega_r t). \tag{12}$$

We next integrate equation (12) along the particle's orbit (6) backward in time to $t = -\infty$, to obtain the particle energy gain from the waves

$$\delta W_A = -\frac{\sqrt{\pi}}{2}\frac{3L^2W}{B_ER_E} \cdot E_\phi k(\tau) g(t,\tau) \exp i(m\phi - m\omega_d t), \tag{13}$$

where we define $k(\tau) = \tau \exp\left[\frac{-(m\omega_d-\omega_r)^2\tau^2}{4}\right]$ and $g(t,\tau) = \mathrm{erf}\left(\frac{t}{\tau} - i\frac{m\omega_d\tau-\omega_r\tau}{2}\right) + 1$. This new equation is much more complicated than equation (7) in the conventional drift resonance theory; however, drift resonance still occurs when $m\omega_d$ equals $\omega_r$. For particles at the resonant energy, $k(\tau)$ reaches its maximum, $\tau$, and the complex $g(t,\tau)$ function degenerates to a real function, $\mathrm{erf}(\frac{t}{\tau})+1$. Therefore, the $\delta W_A$ oscillations near the resonant energy always have the largest amplitude and are always in antiphase with the electric field. These signatures, as discussed before, are consistent with those expected in the conventional theory.

To better understand equation (13), we present in Figure 1 an example of electron interactions with ULF waves during the growth and damping stages. We adopt the following parameters: $\tau = 350$ s, $m = 8$, $L = 4.5$, $E_\phi = 2$ mV/m, the wave period is 300 s, and the corresponding resonant energy is about 250 keV. The azimuthal electric field (11) at a fixed $\phi$ location is presented in Figure 1a, which has the form associated with wave growth before $t = 0$ and wave damping afterward. The corresponding $\delta W_A$ values at the same $\phi$ location, given in equation (13), are shown in Figure 1b as a function of time and electron energy.

During the early growth stage of the wave ($t < -\tau$), the wave amplitude is relatively small; and therefore, the electron energy does not change significantly. The corresponding phase shift of $\delta W_A$ across different energies is also small, forming slightly slanted, faint stripes in Figure 1b. As time proceeds, the electric field oscillations

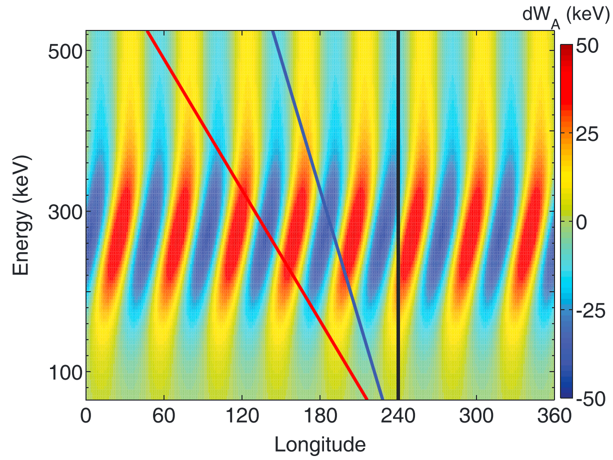


**Figure 2.** Electron energy gain as a function of longitude and energy for an ULF wave whose amplitude peaks at $t = 0$. The black line represents electrons observed by a virtual spacecraft at a fixed $\phi$ at $t = 0$; electrons located along the blue and the red lines at $t = 0$ would reach the spacecraft at $t = 300$ and 600 s, respectively.

and the associated $\delta W_A$ modulations both become stronger, and the phase shift of $\delta W_A$ across energies gradually increases to reach 180° at $t = 0$. These signatures in the wave growth stage, despite being derived from a new equation, are quite similar to those expected from the conventional drift resonance theory. As discussed in *Zhou et al.* [2015], a large $\mathrm{Im}(\omega)$ value in the denominator of equation (7) produces a small phase shift in $\delta W_A$ ($\ll$180°) across energies. In other words, the decreasing $\mathrm{Im}(\omega)$ values in equation (10) would be manifested in the conventional theory by an increase of the phase shift, which reaches 180° when $\mathrm{Im}(\omega)$ decreases to zero at $t = 0$. These features are all qualitatively consistent with the signatures shown in Figure 1b before $t = 0$.

For $t > 0$, the signatures become more complicated and can no longer be approximated by the conventional theory, which does not consider a decaying amplitude of the driving signal. Despite the decreasing wave amplitude, the $\delta W_A$ modulation amplitude continues to increase toward an asymptotic value, which is about 80 keV for resonant electrons. The total phase shift across energies also keeps growing as indicated by increasingly tilted stripes in Figure 1b, even when the wave vanishes at $t \gg \tau$. The continued growth of phase shift can actually be interpreted as an energy-dependent frequency of $\delta W_A$ oscillations, with higher-energy electrons being modulated at a higher frequency. Such an energy dependence can be explained by an approximation of equation (13) at $t \gg \tau$ to

$$\delta W_A \approx -\frac{3\sqrt{\pi}L^2 W}{B_E R_E} \cdot E_\phi k(\tau) \exp i(m\phi - m\omega_d t), \text{ when } t \gg \tau, \tag{14}$$

which clearly indicates that the angular frequency of the $\delta W_A$ modulations is $m\omega_d$, rather than $\omega_r$ as obtained from the conventional theory. The increasingly tilted stripes arise from the energy dependence of the particle drift speed.

To better illustrate the physics behind our interpretation, we follow equation (13) to show in Figure 2 the longitude and energy distributions of $\delta W_A$ at $t = 0$. One can immediately find sectors containing accelerated electrons adjacent to those containing decelerated electrons, which constitute a total of 2 m sectors in the longitudinal-energy space. As we have discussed before, a spacecraft with a fixed $\phi$ location (represented by the black line in Figure 2) would observe a phase shift of 180° between the lowest and the highest energies. If we turn off the wave-associated electric field at this moment, the electron energy distributions at fixed $\phi$ would then be distorted by their energy-dependent drift motion. In other words, at a later time $t > 0$, the spacecraft would observe electrons that were originally located at different, energy-dependent longitudes. For example, electrons originally located at the blue and the red lines would be captured by the spacecraft at $t = 300$ and 600 s, respectively. Therefore, within the same time interval, the spacecraft would observe peaks and troughs of $\delta W_A$ more frequently for electrons with higher energies than for those at lower energies as manifested in Figure 1b.

We next consider the manifestation of wave-produced $\delta W_A$ oscillations observable from a particle detector with a finite energy resolution. The transformation from $\delta W_A$ to $\delta f_A$ is based on equation (8), which shows that $\delta f_A$ and $\delta W_A$ could either be in phase or antiphase depending on the radial profile of $f(L,\mu)$. The radial gradient of $f(L,\mu)$ is traditionally thought to be positive in the outer radiation belt [*Schulz and Lanzerotti*, 1974], although recent observations have suggested that negative gradient may also appear in many occasions [*Chen et al.*, 2007; *Turner et al.*, 2010]. Here we assume, without loss of generality, that the radial gradient of $f(L,\mu)$ is positive. This positive gradient could be set up by adopting a spatially independent power law distribution of background particles, $f \propto W^{-\alpha}$, with the power law exponent $\alpha$ assumed to be 3. We next follow equation (9) to obtain $\delta f_A$ at each energy, before we integrate the resulting $\delta f_A$ values over the width of each energy bin and divide them by the corresponding $f$ values, to define residual PSDs observable from each energy channel of the particle detector.

Figure 1c shows the predicted spectrum of residual phase space density observed by a virtual detector with the same channel widths as the MagEIS (Magnetic Electron Ion Spectrometer) instrument [*Blake et al.*, 2013] on board Van Allen Probes. The residual PSD observations, before $t=0$, are very similar to the $\delta W_A$ signatures given in Figure 1b. However, after $t=0$, the modulation of residual PSD starts to weaken and eventually vanishes despite the increasing amplitude of the $\delta W_A$ modulation. The attenuation of the observable PSD modulations is caused by the phase mixing effect described in *Schulz and Lanzerotti* [1974] due to the acceptance of particles with different energies within a single energy channel of finite width. In other words, the increasing phase differences between particles within the same energy channel imply that the channel will eventually respond to two signals in antiphase, and the overlap between them will cancel out the particle PSD modulations within the energy channel. Similar conclusions were also reached by *Degeling and Rankin* [2008], who investigated drift resonance behavior using numerical simulations. The attenuation could occur even in a shorter time if the detectors have a lower energy resolution than MagEIS, which may explain why drift resonance signatures were seldom reported in spacecraft observations before the Van Allen Probes era [*Mann et al.*, 2013].

Before these signatures of wave-particle interactions are directly compared to Van Allen Probes observations, we note that in Earth's magnetosphere the growth and damping of ULF waves are usually governed by different mechanisms [*Glassmeier et al.*, 1984]. Therefore, the assumption of a single time scale, $\tau$, for the wave growth and the wave damping stages may not be valid. It is more appropriate to assume two different time scales, $\tau_1$ (before $t=0$) and $\tau_2$ (after $t=0$) that correspond to these two stages. The new assumption hardly changes the $\delta W_A$ modulation before $t=0$, except for the replacement of $\tau$ by $\tau_1$ in equation (13). After $t=0$, the $\delta W_A$ modulation becomes

$$\delta W_A = \delta W_{A0}\exp(-im\omega_d t) - \frac{\sqrt{\pi}}{2}\frac{3L^2W}{B_E R_E}\cdot E_\phi k(\tau_2)[g(t,\tau_2)-g(0,\tau_2)]\exp i(m\phi - m\omega_d t), \tag{15}$$

where $\delta W_{A0}$ represents the energy modulation at $t=0$. We next consider a ULF wave event with $\tau_1 = 200$ s and $\tau_2 = 750$ s, and the electron responses to the waves are shown in Figure 3. From this figure one finds that the newly introduced asymmetric wave profile hardly changes the picture of wave-particle interactions. Most of the characteristic signatures in Figure 1 remain valid in Figure 3, especially the increasingly tilted stripes and the gradual attenuation of the PSD oscillations. These characteristic signatures are to be compared in the next section with Van Allen Probes observations.

## 4. Observations

The observational data sets utilized in the comparison are from the Van Allen Probes, with the electric field, magnetic field, and energetic electron data provided by the electric fields and waves [*Wygant et al.*, 2013], the fluxgate magnetometer (MAG) [*Kletzing et al.*, 2013], and the MagEIS [*Blake et al.*, 2013] instruments, respectively. Since the electric field measurements only have two components available during most of the time, we also use the approximation $\boldsymbol{E}\cdot\boldsymbol{B} = 0$ to determine the third electric field component. The magnetic field data are also used to define a mean field-aligned (MFA) coordinate system, in which the parallel (n) direction is the direction of the 15-minute sliding average magnetic field, the azimuthal direction ($\phi$) is parallel to the vector product of the parallel direction and the spacecraft geocentric position vector, and the radial direction (r) completes the triad. Then we project the electric field data to the MFA coordinate, to obtain its azimuthal and radial components associated with the ULF poloidal/compressional and toroidal wave modes, respectively.

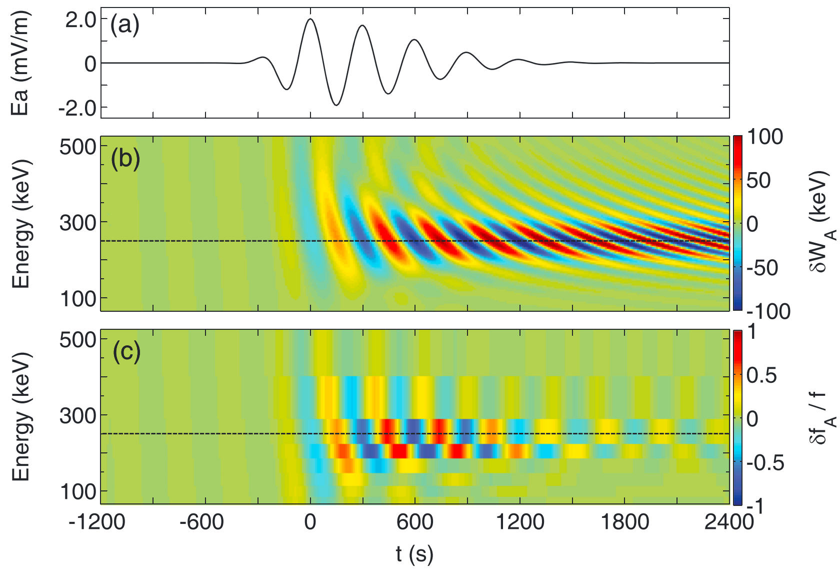


**Figure 3.** Electron responses to ULF waves in the same format as in Figure 1 except that the growth stage of the ULF waves is shorter than the damping stage.

Figure 4 presents a 1 h overview of ULF wave interactions with energetic electrons observed by Van Allen Probes on 11 April 2014. The ULF waves were excited at approximately 0800 UT, presumably by a sudden decrease of the solar wind dynamic pressure (from 3 to 1 nPa, not shown). During this 1 h interval, Van Allen Probe B moved inward ($L^*$ changed from 4.9 to 4.1) in the dayside magnetosphere (Magnetic Local Time (MLT) $\sim$12), and Van Allen Probe A moved outward from $L^*$=4.5 to 5.1 in the morning sector (MLT $\sim$9). Figure 4a shows the azimuthal electric field observed by Van Allen Probe B, which clearly shows an amplitude enhancement of the electric field oscillations (at the period of about 5 min) before the ULF waves started damping at $\sim$0810 UT. The corresponding electron residual PSDs, defined by $(f-f_0)/f_0$ where $f_0$ is a 10 min sliding average of the electron PSD $f$, are shown in Figure 4b for electrons with pitch angles between 57° and 123°.

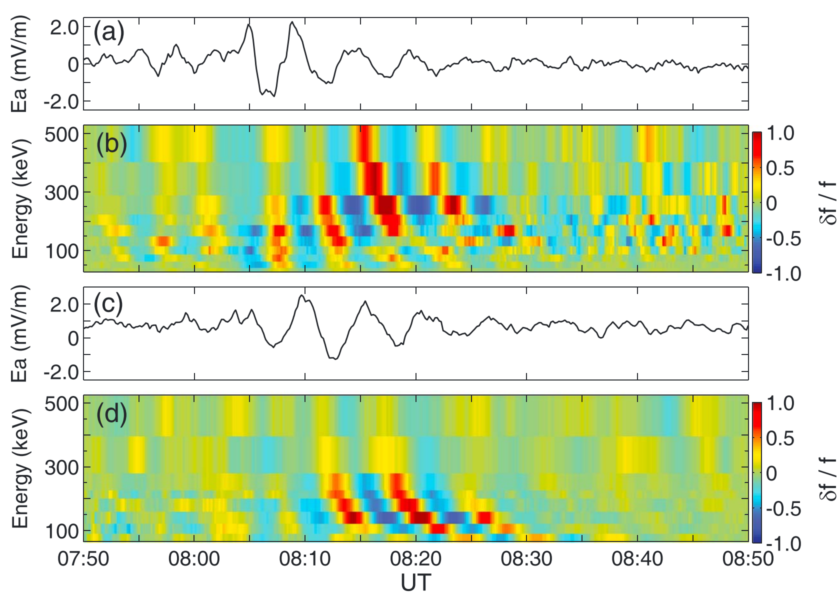


**Figure 4.** Van Allen Probes observations of ULF wave-particle interactions in the inner magnetosphere on 11 April 2014. (a) Azimuthal electric field and (b) residual PSD of energetic electrons observed by Van Allen Probe B. (c and d) Van Allen Probe A observations in the same format as in Figures 4a and 4b.

A striking feature in Figure 4b is the increasingly tilted stripes: the phase shift between the lowest- and the highest-energy channels, initially very small before 0805 UT, gradually increased to ~180° when the wave amplitude peaked at 0810 UT and continued increasing until the eventual attenuation of the PSD oscillations. As we have described before, this is a characteristic signature of particle interaction with ULF waves during a typical wave lifespan. One may also find that the amplitude of the electron residual PSD oscillations peaks at the energy of ~250 keV, which indicates that this is most likely the resonant energy. At this resonant energy, a direct comparison between Figures 4a and 4b shows that the electron residual PSD oscillations are nearly always in antiphase with the electric field, which also agrees with the predicted signatures in the generalized theory of drift resonance.

Van Allen Probe A observations of the azimuthal electric field and the electron residual PSDs are shown in Figures 4c and 4d, respectively. The electron residual PSD oscillations, at the energy of 250 keV, are also in antiphase with the electric field consistent with a resonant wave-particle interaction at this energy. However, the amplitude of the residual PSD oscillations peaks at a lower energy of ~150 keV. This may be caused by a larger $\partial f/\partial W$ ratio at 150 keV than at 250 keV (equation (9)), which amplifies the PSD oscillations more significantly at 150 keV even if the corresponding $\delta W_A$ oscillations are smaller. One may also find that before 0810 UT, the electron spectrum showed faint, nearly vertical stripes indicating a very small phase shift across energy channels. After that, the phase shift increased significantly until the attenuation of the PSD oscillations. Therefore, these signatures also agree with the theoretical predictions described in the previous section.

## 5. Summary and Discussions

The conventional drift resonance theory [*Southwood and Kivelson*, 1981, 1982], with the default assumption of a time independent, positive, and extremely small wave growth rate, has long been applied to understand the particle behavior in ULF wave fields and to interpret observational signatures of ULF wave-particle interactions [*Zong et al.*, 2007; *Claudepierre et al.*, 2013; *Dai et al.*, 2013; *Mann et al.*, 2013; *Degeling et al.*, 2014]. More recently, the strong assumption has been slightly relaxed with the introduction of a large wave growth rate. Such a relaxation does not explicitly change any equations in the theory; however, it predicts very different observational signatures in the particle spectrum, which in a specific case study reconciles many apparent inconsistencies between theory and spacecraft observations [*Zhou et al.*, 2015].

In this paper, we further relax the assumption to allow a time-dependent wave growth rate, which is large and positive in the wave early growth stage and gradually decreases to negative values in the damping stage. This is a natural assumption, because any ULF waves should firstly experience a growth stage to extract energy from external and/or internal sources, and as time proceeds the waves should eventually be damped. We find that in this case, many equations in the conventional drift resonance theory are no longer valid; and therefore, we develop a generalized theory which describes very different particle signatures from those in the conventional theory. In the wave growth stage, the amplitude of the particle PSD oscillations gradually increases, and the phase difference between the lowest- and the highest-energy channels also increases from very small values to 180° when the wave stops growing. After that, despite the decreasing wave amplitude, both the particle PSD oscillation amplitude and the total phase shift across energies continue to increase until the phase mixing effect (due to the limited energy resolution of particle detectors) attenuates the particle PSD oscillations. These predicted signatures are found consistent with Van Allen Probes observations, which validates the generalized drift resonance theory and provides new insights into our understanding of particle dynamics within the entire ULF wave life span.

Finally, we note that the generalized drift resonance theory is derived with several assumptions inherited directly from the conventional theory. A most obvious assumption is that the theory deals with nonrelativistic particles. This assumption overestimates the particle drift velocity (compare equations (2) and (3)) and therefore leads to an overestimation of $\delta W_A$ and an underestimation of the resonant energy. Another important assumption used here is that the particle's drift orbit (equation (6)) remains unperturbed despite its energy gain/loss from the ULF waves. This assumption is appropriate only if the particle energy gain $\delta W_A$ is significantly smaller than its initial energy $W$. In our sample case, however, this assumption is only marginally valid since the $\delta W_A$ value may reach 80 keV at a resonant energy of 250 keV (see Figure 1b). Therefore, for ULF waves with stronger electric field and/or with longer life span, a direct application of the drift resonance theory may become questionable. A more self-consistent analysis should take into account the changes of $W$ (and consequently the changes of $L$ given the conservation of the magnetic moment) of particles during their interactions with the ULF waves. It is also assumed in equation (4), which applies to both the conventional and the generalized theory, that the amplitude of the ULF wave-associated electric field does not depend on magnetic longitude. This is probably not typical in the magnetosphere, and the ULF waves may be confined in a limited range of longitudes [*Liu et al.*, 2009, 2016]. Therefore, we should also take into account in the theoretical framework the longitudinal distributions of the ULF wave power. These extensions, however, are beyond the scope of this paper and will be addressed in a future study.

**Acknowledgments**
We thank Ian Mann, Vassilis Angelopoulos, and Seth Claudepierre for helpful discussions. This study was supported by NSFC grants 41421003 and 41474140. Rankin acknowledges support from the Canadian Space Agency and the National Science and Engineering Research Council of Canada. The Van Allen Probes data used in this paper can be achieved online from NASA's Space Physics Data Facility at http://spdf.gsfc.nasa.gov/.

## References

Allan, W., S. P. White, and E. M. Poulter (1986), Impulse-excited hydromagnetic cavity and field-line resonances in the magnetosphere, *Planet. Space Sci.*, *34*, 371–385, doi:10.1016/0032-0633(86)90144-3.

Blake, J. B., et al. (2013), The Magnetic Electron Ion Spectrometer (MagEIS) instruments aboard the Radiation Belt Storm Probes (RBSP) spacecraft, *Space Sci. Rev.*, *179*, 383–421, doi:10.1007/s11214-013-9991-8.

Chen, L., and A. Hasegawa (1974), A theory of long-period magnetic pulsations: 1. Steady state excitation of field line resonance, *J. Geophys. Res.*, *79*, 1024–1032, doi:10.1029/JA079i007p01024.

Chen, Y., G. D. Reeves, and R. H. W. Friedel (2007), The energization of relativistic electrons in the outer Van Allen radiation belt, *Nat. Phys.*, *3*, 614–617, doi:10.1038/nphys655.

Claudepierre, S. G., et al. (2013), Van Allen Probes observation of localized drift resonance between poloidal mode ultra-low frequency waves and 60 keV electrons, *Geophys. Res. Lett.*, *40*, 4491–4497, doi:10.1002/grl.50901.

Cummings, W. D., R. J. O'Sullivan, and P. J. Coleman Jr. (1969), Standing Alfven waves in the magnetosphere, *J. Geophys. Res.*, *74*, 778–793.

Dai, L., et al. (2013), Excitation of poloidal standing Alfven waves through drift resonance wave-particle interaction, *Geophys. Res. Lett.*, *40*, 4127–4132, doi:10.1002/grl.50800.

Degeling, A. W., and R. Rankin (2008), Resonant drift echoes in electron phase space density produced by dayside Pc5 waves following a geomagnetic storm, *J. Geophys. Res.*, *113*, A10220, doi:10.1029/2008JA013254.

Degeling, A. W., R. Rankin, and Q.-G. Zong (2014), Modeling radiation belt electron acceleration by ULF fast mode waves, launched by solar wind dynamic pressure fluctuations, *J. Geophys. Res. Space Physics*, *119*, 8916–8928, doi:10.1002/2013JA019672.

Elkington, S. R., M. K. Hudson, and A. A. Chan (2003), Resonant acceleration and diffusion of outer zone electrons in an asymmetric geomagnetic field, *J. Geophys. Res.*, *108*, 1116, doi:10.1029/2001JA009202.

Foster, J. C., J. R. Wygant, M. K. Hudson, A. J. Boyd, D. N. Baker, P. J. Erickson, and H. E. Spence (2015), Shock-induced prompt relativistic electron acceleration in the inner magnetosphere, *J. Geophys. Res.*, *120*, 1661–1674, doi:10.1002/2014JA020642.

Glassmeier, K. H., H. Volpers, and W. Baumjohann (1984), Ionospheric Joule dissipation as a damping mechanism for high latitude ULF pulsations—Observational evidence, *Planet. Space Sci.*, *32*, 1463–1466, doi:10.1016/0032-0633(84)90088-6.

Hao, Y. X., et al. (2014), Interactions of energetic electrons with ULF waves triggered by interplanetary shock: Van Allen Probes observations in the magnetotail, *J. Geophys. Res. Space Physics*, *119*, 8262–8273, doi:10.1002/2014JA020023.

Hartinger, M., V. Angelopoulos, M. B. Moldwin, K.-H. Glassmeier, and Y. Nishimura (2011), Global energy transfer during a magnetospheric field line resonance, *Geophys. Res. Lett.*, *38*, L12101, doi:10.1029/2011GL047846.

Hsu, T.-S., and R. L. McPherron (2007), A statistical study of the relation of Pi 2 and plasma flows in the tail, *J. Geophys. Res.*, *112*, A05209, doi:10.1029/2006JA011782.

Kepko, L., H. E. Spence, and H. J. Singer (2002), ULF waves in the solar wind as direct drivers of magnetospheric pulsations, *Geophys. Res. Lett.*, *29*, 1197, doi:10.1029/2001GL014405.

Kletzing, C. A., et al. (2013), The Electric and Magnetic Field Instrument Suite and Integrated Science (EMFISIS) on RBSP, *Space Sci. Rev.*, *179*, 127–181, doi:10.1007/s11214-013-9993-6.

Kokubun, S., M. G. Kivelson, R. L. McPherron, and C. T. Russell (1977), OGO 5 observations of Pc 5 waves: Particle flux modulations, *J. Geophys. Res.*, *82*, 2774–2786.

Lee, D.-H., and R. L. Lysak (1989), Magnetospheric ULF wave coupling in the dipole model—The impulsive excitation, *J. Geophys. Res.*, *94*, 17,097–17,103, doi:10.1029/JA094iA12p17097.

Liu, W., T. E. Sarris, X. Li, S. R. Elkington, R. Ergun, V. Angelopoulos, J. Bonnell, and K. H. Glassmeier (2009), Electric and magnetic field observations of Pc4 and Pc5 pulsations in the inner magnetosphere: A statistical study, *J. Geophys. Res.*, *114*, A12206, doi:10.1029/2009JA014243.

Liu, W., W. Tu, X. Li, T. Sarris, Y. Khotyaintsev, H. Fu, H. Zhang, and Q. Shi (2016), On the calculation of electric diffusion coefficient of radiation belt electrons with in situ electric field measurements by THEMIS, *Geophys. Res. Lett.*, *43*, 1023–1030, doi:10.1002/2015GL067398.

Mann, I. R., et al. (2013), Discovery of the action of a geophysical synchrotron in the Earth's Van Allen radiation belts, *Nat. Comm.*, *4*, 2795, doi:10.1038/ncomms3795.

Mathie, R. A., and I. R. Mann (2001), On the solar wind control of Pc5 ULF pulsation power at mid-latitudes: Implications for MeV electron acceleration in the outer radiation belt, *J. Geophys. Res.*, *106*, 29,783–29,796, doi:10.1029/2001JA000002.

Northrop, T. G. (1963), Adiabatic charged-particle motion, *Rev. Geophys.*, *1*, 283–304, doi:10.1029/RG001i003p00283.

Olson, J. V. (1999), Pi2 pulsations and substorm onsets: A review, *J. Geophys. Res.*, *104*, 17,499–17,520, doi:10.1029/1999JA900086.

Schulz, M., and L. J. Lanzerotti (1974), Particle diffusion in the radiation belts, in *Physics and Chemistry in Space*, vol. 7, p. 215, Springer, New York.

Shen, X. C., et al. (2015), Magnetospheric ULF waves with increasing amplitude related to solar wind dynamic pressure changes: The Time History of Events and Macroscale Interactions during Substorms (THEMIS) observations, *J. Geophys. Res. Space Physics*, *120*, 7179–7190, doi:10.1002/2014JA020913.

Shi, Q. Q., et al. (2013), THEMIS observations of ULF wave excitation in the nightside plasma sheet during sudden impulse events, *J. Geophys. Res. Space Physics*, *118*, 284–298, doi:10.1029/2012JA017984.

Singer, H. J., W. J. Hughes, and C. T. Russell (1982), Standing hydromagnetic waves observed by ISEE 1 and 2—Radial extent and harmonic, *J. Geophys. Res.*, *87*, 3519–3529, doi:10.1029/JA087iA05p03519.

Southwood, D. J. (1974), Some features of field line resonances in the magnetosphere, *Planet. Space Sci.*, *22*, 483–491, doi:10.1016/0032-0633(74)90078-6.

Southwood, D. J., and M. G. Kivelson (1981), Charged particle behavior in low-frequency geomagnetic pulsations: I. Transverse waves, *J. Geophys. Res.*, *86*, 5643–5655.

Southwood, D. J., and M. G. Kivelson (1982), Charged particle behavior in low-frequency geomagnetic pulsations. II. Graphical approach, *J. Geophys. Res.*, *87*, 1707–1710.

Southwood, D. J., J. W. Dungey, and R. J. Etherington (1969), Bounce resonant interaction between pulsations and trapped particles, *Planet. Space Sci.*, *17*, 349–361, doi:10.1016/0032-0633(69)90068-3.

Takahashi, K., and R. L. McPherron (1984), Standing hydromagnetic oscillations in the magnetosphere, *Planet. Space Sci.*, *32*, 1343–1359.

Turner, D. L., X. Li, G. D. Reeves, and H. J. Singer (2010), On phase space density radial gradients of Earth's outer-belt electrons prior to sudden solar wind pressure enhancements: Results from distinctive events and a superposed epoch analysis, *J. Geophys. Res.*, *115*, A01205, doi:10.1029/2009JA014423.

Wygant, J. R., et al. (2013), The electric field and waves instruments on the Radiation Belt Storm Probes mission, *Space Sci. Rev.*, *179*, 183–220, doi:10.1007/s11214-013-0013-7.

Zhou, X.-Z., et al. (2015), Imprints of impulse-excited hydromagnetic waves on electrons in the Van Allen radiation belts, *Geophys. Res. Lett.*, *42*, 6199–6204, doi:10.1002/2015GL064988.

Zong, Q.-G., et al. (2007), Ultralow frequency modulation of energetic particles in the dayside magnetosphere, *Geophys. Res. Lett.*, *34*, L12105, doi:10.1029/2007GL029915.

Zong, Q.-G., et al. (2009), Energetic electron response to ULF waves induced by interplanetary shocks in the outer radiation belt, *J. Geophys. Res.*, *114*, A10204, doi:10.1029/2009JA014393.

## Erratum

Equation (15) in the originally published version of this paper included an error: the first term in the right-hand side, $\delta W_{A0}$, should have been multiplied by $\exp(-im\omega_d t)$. This error has since been corrected, and this version may be considered the authoritative version of record. The authors thank Ms. Li Li for pointing out this error.